ORIGINAL RESEARCH

Characterization of Distinct Macrophage Subpopulations during Nitrogen Mustard–Induced Lung Injury and Fibrosis

Alessandro Venosa[1], Rama Malaviya[1], Hyejeong Choi[1], Andrew J. Gow[1], Jeffrey D. Laskin[2], and Debra L. Laskin[1]

[1]Departments of Pharmacology and Toxicology, Ernest Mario School of Pharmacy, and [2]Environmental and Occupational Medicine, Robert Wood Johnson Medical School, Rutgers University, Piscataway, New Jersey

Abstract

Nitrogen mustard (NM) is an alkylating agent known to cause extensive pulmonary injury progressing to fibrosis. This is accompanied by a persistent macrophage inflammatory response. In these studies, we characterized the phenotype of macrophages accumulating in the lung over time following NM exposure. Treatment of rats with NM (0.125 mg/kg, intratracheally) resulted in an increase in $CD11b^+$ macrophages in histologic sections. These cells consisted of inducible nitric oxide synthase$^+$ (iNOS) proinflammatory M1 macrophages, and $CD68^+$, $CD163^+$, $CD206^+$, YM-1^+, and arginase-II^+antiinflammatory M2 macrophages. Although M1 macrophages were prominent 1–3 days after NM, M2 macrophages were most notable at 28 days. At this time, they were enlarged and vacuolated, consistent with a profibrotic phenotype. Flow cytometric analysis of isolated lung macrophages identified three phenotypically distinct subpopulations: mature $CD11b^-$, $CD43^-$, and $CD68^+$ resident macrophages, which decreased in numbers after NM; and two infiltrating ($CD11b^+$) macrophage subsets: immature $CD43^+$ M1 macrophages and mature $CD43^-$ M2 macrophages, which increased sequentially. Time-related increases in M1 (iNOS, IL-12α, COX-2, TNF-α, matrix metalloproteinase-9, matrix metalloproteinase-10) and M2 (IL-10, pentraxin-2, connective tissue growth factor, ApoE) genes, as well as chemokines/chemokine receptors associated with trafficking of M1 (CCR2, CCR5, CCL2, CCL5) and M2 (CX_3CR1, fractalkine) macrophages to sites of injury, were also noted in macrophages isolated from the lung after NM. The appearance of M1 and M2 macrophages in the lung correlated with NM-induced acute injury and the development of fibrosis, suggesting a potential role of these macrophage subpopulations in the pathogenic response to NM.

Keywords: nitrogen mustard; macrophages; inflammation; fibrosis

Clinical Relevance

Subsets of activated macrophages are known to participate in both the initiation and resolution of inflammatory responses. However, when overactivated, these cells release excessive quantities of mediators that promote inflammation, tissue injury, and fibrosis. The current studies demonstrate that proinflammatory/cytotoxic (M1) and antiinflammatory/profibrotic (M2) macrophages accumulate sequentially in the lung after nitrogen mustard exposure. Targeting these macrophage subsets may be useful as a novel therapeutic strategy against vesicant-induced lung injury.

Sulfur mustard and the related analog, nitrogen mustard (NM), are highly toxic vesicants developed originally as chemical warfare agents (1, 2). Pulmonary exposure to these vesicants results in extensive tissue damage and persistent bronchiolitis, which progresses to fibrosis (3, 4). Mortality and long-term morbidity following exposure to mustards are a consequence of alkylation and crosslinking of critical nucleophilic sites in target tissues including DNA and proteins. This

(Received in original form April 9, 2015; accepted in final form August 10, 2015)

This work was supported by National Institutes of Health grants U54AR055073, R01ES004738, R01CA132624, P30ES005022, K01HL096426, and R01HL086621.

Author Contributions: A.V., R.M., and D.L.L. contributed to the conception and design; A.V. contributed to the performing of the experiments; A.V., H.C., A.J.G., J.D.L., and D.L.L. contributed to the data analysis and interpretation; A.V. and D.L.L. contributed to the drafting of the manuscript; A.V., A.J.G., J.D.L., and D.L.L. contributed to the editing and revision of the manuscript; all authors contributed to approval of the final submitted version.

Correspondence and requests for reprints should be addressed to Debra L. Laskin, Ph.D., Department of Pharmacology and Toxicology, Ernest Mario School of Pharmacy, Rutgers University, 160 Frelinghuysen Road, Piscataway, NJ 08854. E-mail: laskin@eohsi.rutgers.edu

This article has an online supplement, which is accessible from this issues's table of contents at www.atsjournals.org

Am J Respir Cell Mol Biol Vol 54, Iss 3, pp 436–446, Mar 2016

Originally Published in Press as DOI:10.1165/rcmb.2015-0120OC on August 14, 2015
Internet address: www.atsjournals.org

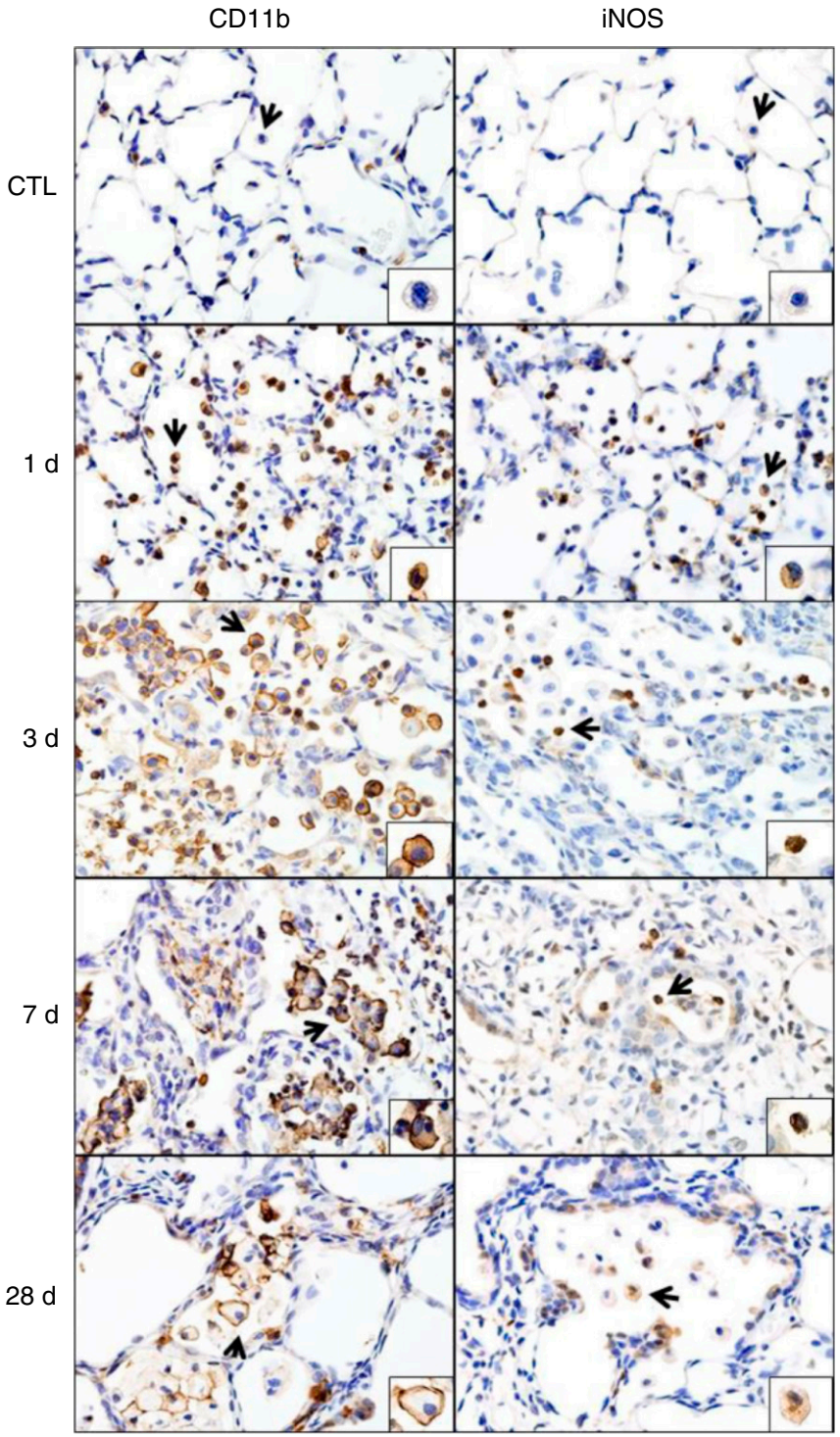

Figure 1. Effects of nitrogen mustard (NM) on CD11b and inducible nitric oxide synthase (iNOS) expression. Lung sections, prepared 1, 3, 7, and 28 days (d) after exposure of rats to phosphate-buffered saline control (CTL) or NM, were immunostained with antibodies to CD11b or iNOS. Binding was visualized using a Vectastain kit. *Arrows* indicate macrophage in insets. Original magnification, 60×; inset magnification, 200×. Representative sections from three rats/treatment group are shown.

combination of protein and DNA modification, along with direct oxidative action, leads to cytotoxicity and inflammation, which contribute to tissue injury (4).

Pulmonary injury induced by mustards is associated with an accumulation of activated macrophages in the lung (5–7). These cells are known to play a role in both acute and chronic pulmonary pathologies, including cytotoxicity and fibrosis (8). Evidence suggests that these activities are mediated by distinct subpopulations of macrophages, which develop in response to inflammatory signals they encounter in the tissue microenvironment (9). Two major phenotypically distinct macrophage subpopulations have been identified which have been characterized broadly as proinflammatory/cytotoxic M1 macrophages and antiinflammatory/wound repair M2 macrophages (10). Although early in the pathogenic response to toxicants, M1 macrophages release mediators aimed at eliminating foreign materials and debris, later in the process, M2 macrophages appear in the tissue, releasing mediators that down-regulate the inflammatory response and promote the resolution of injury and wound repair (11). M2 macrophages can be further divided into subpopulations that play different roles in regulating inflammation and wound repair. These include M2a macrophages, which promote type-II immune responses and fibrogenesis, M2b macrophages, which are immunoregulatory, and M2c macrophages, which are antiinflammatory and initiate tissue remodeling (9, 10). Prolonged activation and excessive release of mediators by M1 and/or M2 macrophages can contribute to tissue injury and disease pathogenesis and to the development of fibrosis (12). The key to an effective inflammatory response to an insult appears to be balanced activation of the two macrophage populations. In the current studies, we used techniques in immunohistochemistry and flow cytometry to characterize activated macrophages accumulating in the lung following exposure of rats to vesicants, using NM as a model. Our findings that M1 and M2 macrophages sequentially accumulate in the lung following NM exposure, and that their appearance correlates with acute injury and fibrosis, suggest that they may contribute to these pathogenic responses.

Materials and Methods

Animals, Treatments, and Sample Collection

Male Wistar rats (8 wk old, 225–250 g; Harlan Laboratories, Indianapolis, IN), were housed in microisolation cages and provided food and water *ad libitum*. The animals were anesthetized by intraperitoneal ketamine (80 mg/kg) and xylazine (10 mg/kg) and then administered phosphate-buffered saline (PBS) or freshly prepared NM (0.125 mg/kg, mechlorethamine hydrochloride, Sigma-Aldrich, St. Louis, MO) intratracheally (13). In earlier studies, we found that this dose of NM is effective in inducing acute lung injury, which progresses to fibrosis without significant mortality (6). The animals were killed with sodium pentobarbital (50 mg/kg, intraperitoneally) after 1–28 days. Bronchoalveolar lavage fluid (BAL) was collected by slowly instilling and withdrawing 10 ml ice-cold PBS into the lung through a tracheal cannula. This procedure had no effect on the macrophage populations in the lung (*see* Figure E1 in the online supplement). BAL was centrifuged (300 × *g*, 8 min, and cell and protein content was assayed (6). The lung was then removed, and 10 ml PBS was instilled and withdrawn four times while gently massaging the tissue. The cell suspension was combined with the initial BAL cells, centrifuged (300 × *g*, 8 min), and viable cells enumerated.

Immunohistochemistry

Following BAL collection, the lung was removed, fixed with 2% paraformaldehyde and paraffin embedded. Sections (5 μm) were deparaffinized with xylene followed by decreasing concentrations of ethanol (100–50%) and then water. After antigen retrieval (10.2 mM sodium citrate, 0.05% Tween 20, pH 6.0, 10 min) and quenching of endogenous peroxidase (3% H_2O_2 in methanol, 30 min), sections were incubated at room temperature with 10% serum and then overnight (4°C) with primary antibodies or serum/IgG controls (Table E1). Sections were then washed and incubated (30 min) with biotinylated secondary antibody (Vectastain Elite ABC kit; Vector Laboratories, Burlingame, CA); binding was visualized using a Peroxidase DAB Substrate Kit (Vectastain). Random sections from at least three rats/group were analyzed.

Reverse Transcriptase–Polymerase Chain Reaction

mRNA, extracted from lung macrophages using an RNeasy Mini kit (Qiagen, Valencia, CA), was reverse transcribed using a high-capacity complementary DNA (cDNA) reverse transcription kit (Applied Biosystems, Foster City, CA). Standard curves were generated using serial dilutions from pooled cDNA samples. Reverse transcriptase–polymerase chain reaction (PCR) was performed using the SYBR Green PCR Master Mix (Applied Biosystems) on an Applied Biosystems 7300HT thermocycler. Glyceraldehyde 3-phosphate dehydrogenase (GAPDH) was used to normalize the data. Primer sequences are shown in Table E2.

Flow Cytometry/Cell Sorting

Lung cells were incubated with anti–rat-FcRII/III antibody, followed by fluorescently labeled anti-CD11b and CD43 or CD68 antibodies, or appropriate isotype controls (Table E3). In some experiments, the cells were permeabilized and analyzed for Ki67 expression. After fixing in 2% paraformaldehyde, the cells were analyzed on a Gallios flow cytometer (Beckman Coulter Inc., Brea, CA); data were analyzed using Kaluza software (Beckman Coulter Inc.). For sorting, 4′,6-diamidino-2-phenylindole was added

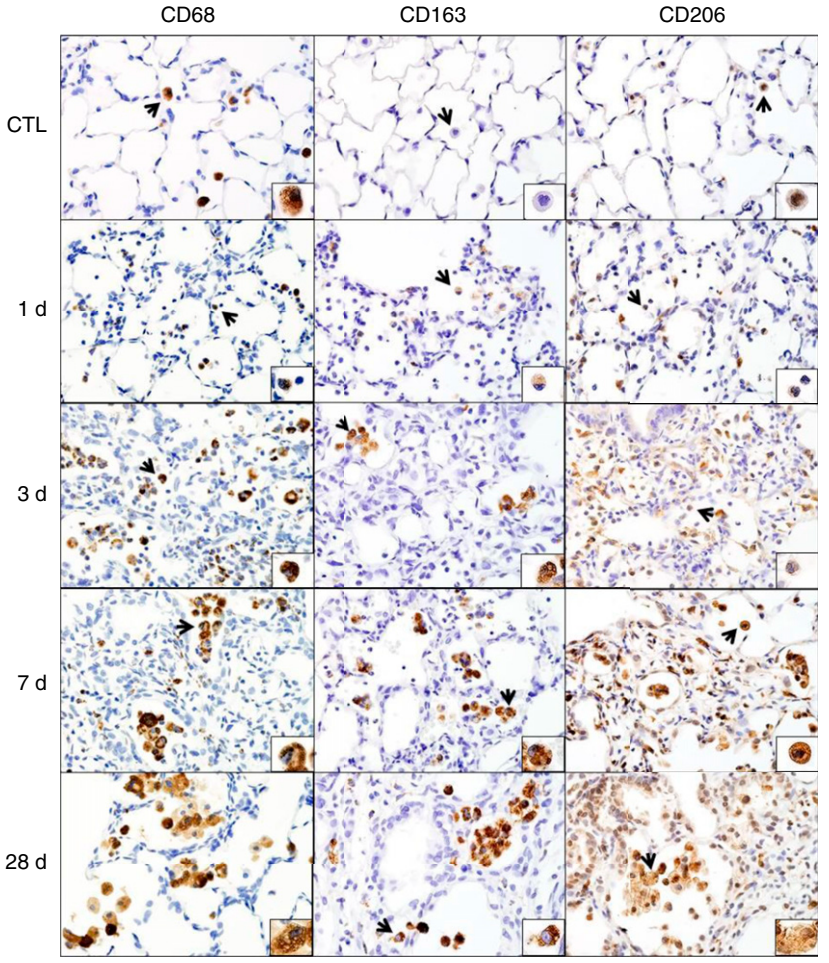

Figure 2. Effects of NM on CD68, CD163, and CD206 expression. Lung sections, prepared 1, 3, 7, and 28 days after exposure of rats to PBS CTL or NM, were immunostained with antibodies to CD68, CD206, or CD163. Binding was visualized using a Vectastain kit. *Arrows* indicate macrophage in insets. Original magnification, 60×; inset magnification, 200×. Representative sections from three rats/treatment group are shown.

to the cell suspension immediately before analysis. Viable cells were sorted into $CD11b^-$/$CD43^-$, $CD11b^+$/$CD43^+$, and $CD11b^+$/$CD43^-$ subpopulations using a MoFlo XDP cell sorter (Beckman Coulter Inc.) and were processed immediately for RNA isolation.

Statistical Analysis

A minimum of three to four animals/group were used. Data were analyzed using one-way analysis of variance with unpaired *t* test or Brown-Forsythe post hoc tests; $P \leq 0.05$ was considered significant.

Results

Macrophages accumulating in the lung after NM were initially characterized *in situ* by immunohistochemistry. CD11b is a β-2 integrin expressed on phagocytic leukocytes infiltrating into areas of tissue damage (14, 15). Following NM exposure, we noted a rapid (<1 d) accumulation of $CD11b^+$ cells in the lung, which persisted for at least 28 days, although at this time the intensity of CD11b expression was reduced (Figure 1 and Table E4). CD11b was also up-regulated in the alveolar epithelium after NM; however, by 28 days, CD11b expression was at control levels. To assess the phenotype of lung macrophages, we analyzed expression of prototypic markers of M1 and M2 macrophages. Exposure of rats to NM was associated with increases in inducible nitric oxide synthase $(iNOS)^+$ M1 macrophages in the lung (Figure 1, *right panels*). This was most prominent 1 day after exposure; subsequently, numbers of $iNOS^+$ cells declined. CD68, CD163, and CD206 are scavenger receptors expressed on M2 macrophages (10, 16). In control rats, resident alveolar macrophages were found to express CD68 and CD206, but not CD163 (Figure 2). NM exposure resulted in a time-related increase in numbers of $CD68^+$, $CD163^+$, and $CD206^+$ macrophages in the lung, as well as in the intensity of expression of these antigens (Table E4). At 1 day after exposure, positively stained cells were small and round; however, by 3 days, these cells had begun to increase in size; this continued for at least 28 days. At this time, the cells appeared vacuolated and were mainly clustered in the airspaces adjacent to fibrotic areas. Expression of two additional markers of an M2 phenotype, arginase-II

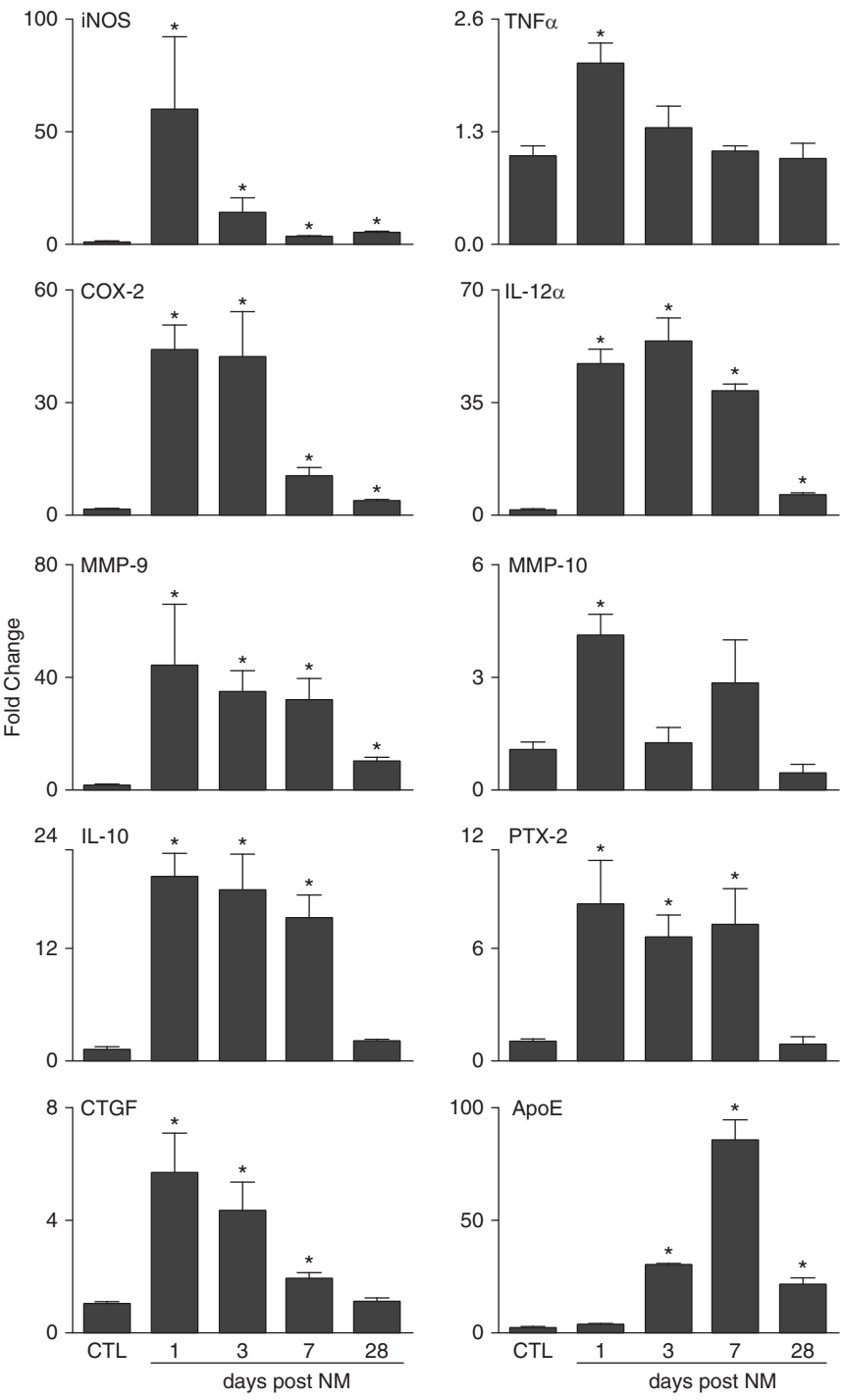

Figure 3. Effects of NM on lung macrophage expression of M1 and M2 genes. Lung macrophages, isolated 1, 3, 7, and 28 days after exposure of rats to PBS CTL or NM, were analyzed for gene expression by RT-PCR. Data were normalized relative to glyceraldehyde 3-phosphate dehydrogenase and presented as fold change relative to CTL. *Error bars*, mean ± SE ($n = 3$–5 rats). *Significantly different ($P \leq 0.05$) from CTL. ApoE, apolipoprotein E; COX, cyclooxygenase; CTGF, connective tissue growth factor; MMP, matrix metalloproteinase; PTX, pentraxin.

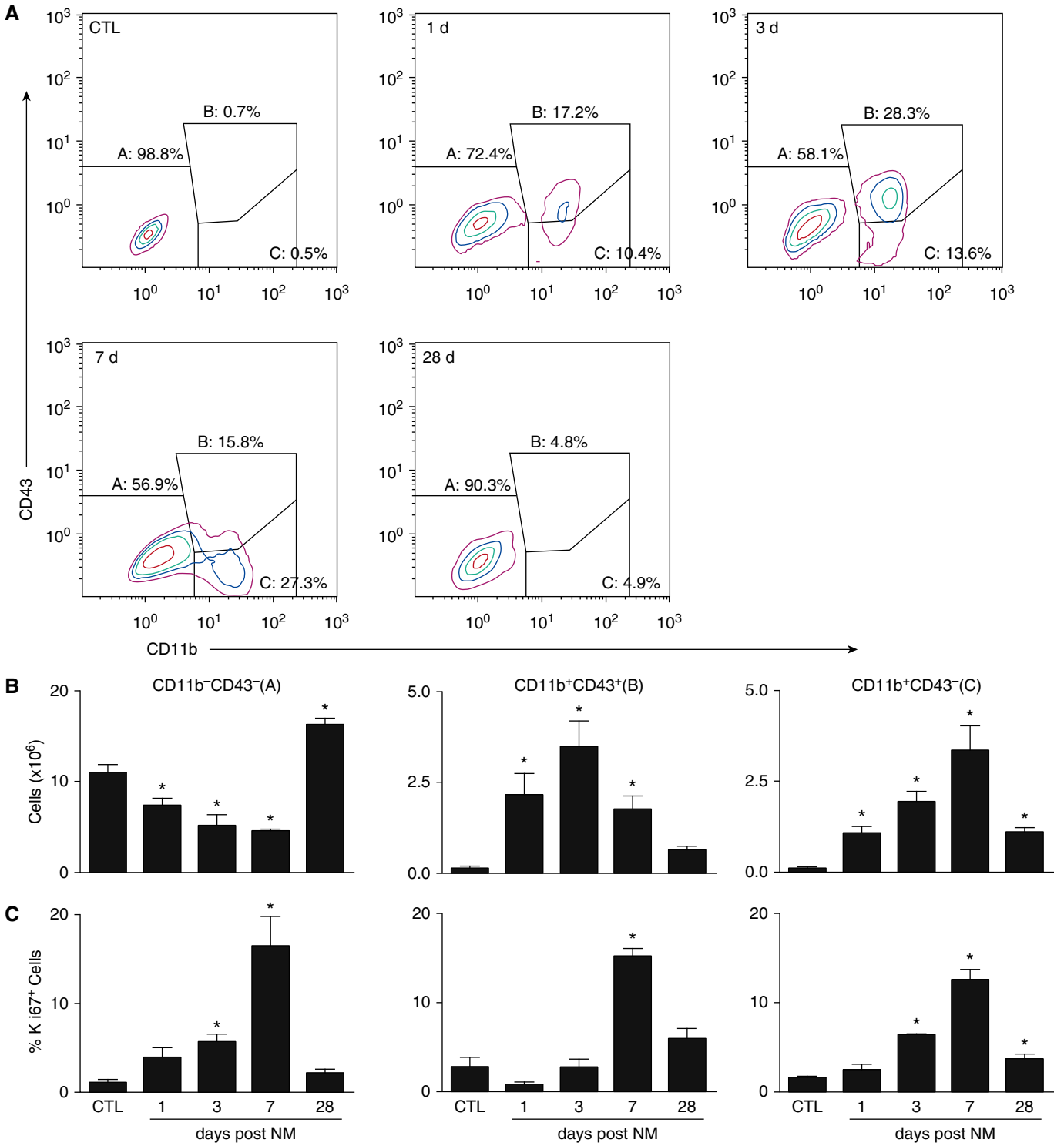

Figure 4. Flow cytometric analysis of lung macrophages. Macrophages, isolated 1, 3, 7, and 28 days after exposure of rats to PBS CTL or NM, were incubated with anti–rat-FcRII/III antibody (1 μl/10^6 cells) for 10 minutes at 4°C, followed by incubation (30 min) with AlexaFluor 488 (AF488) anti-CD11b and AF647 anti-CD43 antibodies or appropriate isotype controls, and then with eFluor780 viability dye (30 min). Cells were then analyzed by flow cytometry. Macrophages were identified based on forward and side scatter followed by doublet discrimination of live cells. (*A*) Representative contour plot showing resident alveolar macrophages (*A*; $CD11b^-CD43^-$), infiltrating immature macrophages (*B*; $CD11b^+CD43^+$), and infiltrating mature macrophages (*C*; $CD11b^+CD43^-$). (*B*) Numbers of $CD11b^-CD43^-$, $CD11b^+CD43^+$, and $CD11b^+CD43^-$ cells were calculated from the percentage of positive macrophages relative to the total number of lung cells recovered. (*C*) Following labeling with CD11b, CD43, and viability dye, cells were incubated for 30 minutes in Fixation/Permeabilization buffer (eBioscience, San Diego, CA), followed by 30 minutes of incubation with eFluor450 Ki67 antibody. Cells were then fixed in 2% paraformahaldehyde and analyzed by flow cytometry. *Error bars,* mean ± SE ($n = 3$–5 rats). *Significantly different ($P \leq 0.05$) from CTL.

Table 1. Expression of CD43 and CD68 by Lung Macrophages

Macrophages	Phenotype	Cells ($\times 10^6$) CTL	Cells ($\times 10^6$) NM
Resident ($CD11b^-$)	$CD43^-$	10.8 ± 0.9	5.2 ± 1.2*
	$CD43^+$	ND	ND
	$CD68^-$	0.5 ± 0.1	1.0 ± 0.1*
	$CD68^+$	9.9 ± 0.1	3.0 ± 0.6*
Infiltrating ($CD11b^+$)	$CD43^-$	0.2 ± 0.1	2.1 ± 0.4*
	$CD43^+$	0.1 ± 0.1	2.7 ± 0.6*
	$CD68^-$	ND	1.0 ± 0.4*
	$CD68^+$	0.1 ± 0.01	2.5 ± 0.5*

Definition of abbreviations: AF, AlexaFluor; CTL, control; ND, not detectable; NM, nitrogen mustard. Cells, isolated 3 days after exposure of rats to PBS CTL or NM, were incubated with AF488 anti-CD11b and AF647 anti-CD43, or AF647 anti-CD68 antibodies. Number of resident ($CD11b^-$) and infiltrating ($CD11b^+$) macrophages expressing CD43 and CD68 were then calculated by flow cytometry based on forward and side scatter followed by doublet discrimination of live cells, relative to the total number of lung cells recovered. Data are presented as mean ± SE ($n = 3$–4 rats).
*Significantly different ($P \leq 0.05$) from CTL rats.

(ARG-II) and YM-1, was also analyzed. Within 1 day of NM, a prominent increase in small $ARG\text{-}II^+$ macrophages was noted in the lung (Figure E2, *left panels*). Low-level ARG-II staining was also observed in the alveolar epithelium. With time, following NM exposure, macrophages staining positively for ARG-II became enlarged and by 28 days, these cells appeared in clusters. $YM\text{-}1^+$ macrophages also increased in the lung after NM, but their appearance was delayed for 3 days. As observed with $ARG\text{-}II^+$ macrophages, by 28 days, clusters of enlarged $YM\text{-}1^+$ macrophages were evident in the lung (Figure E2, *right panels*).

Expression of genes associated with M1 and M2 phenotypes was next analyzed in isolated lung macrophages. M1-associated genes including iNOS, tumor necrosis factor (TNF)-α, COX-2, IL-12α, matrix metalloproteinase (MMP)-9, and MMP-10 (10, 16, 17), were up-regulated in macrophages within 1 day of NM exposure (Figure 3). Increases in TNF-α and MMP-10 were transient, decreasing to control levels by 3 days, but iNOS, COX-2, IL-12α, and MMP-9 remained significantly elevated for at least 28 days, although at reduced levels. NM exposure also resulted in increased expression of genes associated with M2 macrophages; these included IL-10, pentraxin-2 (PTX-2), and connective tissue growth factor (CTGF) (10, 18). Expression of each of these genes increased rapidly (<1 d) in lung macrophages after NM exposure and persisted for at least 7 days; by 28 days, expression was similar to that of the control (Figure 3). We also analyzed the expression of ApoE, which has been shown to dampen M1-driven gene expression and enhance M2 macrophage activation (19). Following NM exposure, ApoE expression increased significantly, peaking at 7 days (Figure 3).

Flow cytometry was used next to characterize the macrophages responding to NM. The majority (~98%) of macrophages from control rats were $CD11b^-$ $CD43^-$ and $CD68^+$ (Figure 4A and Table 1), consistent with a mature resident macrophage phenotype (20, 21). Although numbers of resident macrophages decreased following NM exposure, $CD11b^+$ infiltrating cells increased (Figure 4B and Table 1). $CD11b^+$ cells were found to consist of two subpopulations: $CD43^+$ and $CD43^-$ macrophages (Figures 4A and 4B). Although maximal numbers of $CD11b^+CD43^+$ macrophages were observed in the lung after 3 days, $CD11b^+CD43^-$ macrophages peaked at 7 days. $CD11b^+CD68^+$ macrophages also increased in the lung 3 days after exposure to NM (Table 1). At 28 days, only a small number of $CD11b^+$ infiltrating macrophages were present in the lung, and these cells were mainly $CD43^-$ macrophages. To assess whether increases in $CD11b^+$ macrophages were due to proliferation, we analyzed Ki67 expression (22). In control rats, ~2% of resident $CD11b^-CD43^-$ macrophages were found to be proliferating (Figure 4C). Following NM exposure, proliferation of these cells increased up to 7 days, returning to control levels by 28 days. Increased proliferation of both mature and immature $CD11b^+$ lung macrophages was also observed after NM; this was evident within 3 days in $CD43^-$ infiltrating macrophages, but was delayed for 7 days in $CD43^+$ infiltrating macrophages.

To further characterize these subpopulations, resident and infiltrating macrophages were sorted and examined for relative expression of M1 and M2 genes. RT-PCR analysis showed that 3 days after

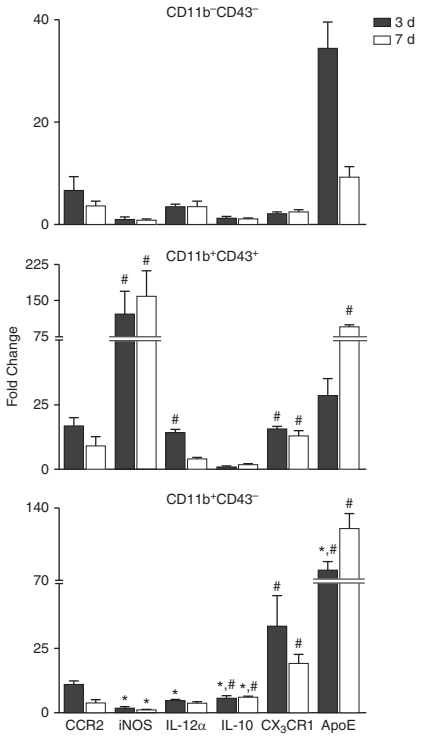

Figure 5. Effects of NM on macrophage subpopulation gene expression. Macrophages, isolated 3 and 7 days after exposure of rats to PBS CTL or NM, were incubated with anti–rat-FcRII/III antibody, and then stained with antibodies to CD11b and CD43 as described in the Figure 4 legend. Viable cells ($DAPI^-$) were sorted into $CD11b^-CD43^-$, $CD11b^+CD43^+$, and $CD11b^+CD43^-$ subpopulations and processed immediately for RT-PCR analysis of expression of pro- (CCR2, iNOS, IL-12α) and anti- (IL-10, CX_3CR1, ApoE) inflammatory genes. Data were normalized to glyceraldehyde 3-phosphate dehydrogenase and presented as fold change relative to resident $CD11b^-CD43^-$ macrophages from CTL rats. *Error bars,* mean ± SE ($n = 3$–4 rats). *Significantly different ($P \leq 0.05$) from $CD11b^+CD43^+$ macrophages. #Significantly different ($P \leq 0.05$) from $CD11b^-CD43^-$ macrophages.

Table 2. Effects of NM on Macrophage Chemokine/Chemokine Receptor Expression

Gene	Days after NM			
	1	3	7	28
CCR2	226.2 ± 36.2*	245.4 ± 45.7*	70.7 ± 12.6*	3.6 ± 1.0*
CCL2	47.8 ± 10.7*	33.8 ± 5.2*	16.4 ± 1.7*	3.0 ± 0.4*
CCR5	147.6 ± 20.1*	188.3 ± 23.6*	88.5 ± 13.7*	4.3 ± 0.7*
CCL5	66.1 ± 15.7*	89.1 ± 9.4*	37.8 ± 1.7*	1.9 ± 0.5
CX_3CR1	17.0 ± 3.6*	17.5 ± 1.1*	18.7 ± 4.0*	1.9 ± 0.1
Fractalkine	4.2 ± 0.5*	2.7 ± 0.5*	3.5 ± 1.2*	1.0 ± 0.4

Definition of abbreviation: NM, nitrogen mustard.
Macrophages, isolated 1, 3, 7, and 28 days after exposure of rats to PBS control or NM, were analyzed by real-time polymerase chain reaction. Data were normalized to glyceraldehyde 3-phosphate dehydrogenase and presented as fold change relative to PBS control. Data were presented as mean ± SE (n = 3–5 rats).
*Significantly different ($P < 0.05$) from control.

NM exposure, M1 (iNOS, IL-12α) gene expression was greater in $CD11b^+CD43^+$ infiltrating macrophages than in resident macrophages or $CD11b^+CD43^-$ infiltrating macrophages (Figure 5); there was also a trend toward increased CCR2 expression. By comparison, $CD11b^+CD43^-$ macrophages expressed greater levels of IL-10, CX_3CR1, and ApoE than did resident or $CD43^+$ infiltrating macrophages. In general, these differences in gene expression between the cells persisted for 7 days, with the exception of ApoE, which was significantly increased at this time in $CD11b^+CD43^+$ macrophages, and IL-12α, which was at control levels (Figure 5).

Macrophage trafficking to sites of injury is mediated by chemokines and chemokine receptors (23). Whereas proinflammatory M1 macrophages accumulate in tissues in response to chemokines CCL2 and CCL5 and express chemokine receptors CCR2 and CCR5, fractalkine and CX_3CR1 are involved in M2 macrophage migration (24). Treatment of rats with NM resulted in increased expression of the M1 chemokine receptors CCR2 and CCR5 and their respective ligands, CCL2 and CCL5, in lung macrophages, which was maximal at 1–3 days (Table 2). Expression of CX_3CR1 and its ligand, fractalkine, also increased rapidly after NM (<1 d) and remained elevated for at least 7 days. Up-regulation of CCR2 and CX_3CR1 mRNA in lung macrophages following NM exposure was correlated with increased protein expression in histological sections. Thus, within 1 day of NM exposure, positively staining CCR2 and CX_3CR1 macrophages were identified in the lung (Figure 6). By 3 days, staining was also up-regulated in epithelial cells, which persisted for 28 days.

Discussion

NM-induced lung injury and fibrosis are associated with increased numbers of macrophages in peribronchial and perivascular regions of the lung (6). The current studies demonstrate that these cells consist of subpopulations of $CD11b^+$ infiltrating macrophages exhibiting M1 and M2 phenotypes. Whereas overactive M1 macrophages release cytotoxic/proinflammatory mediators that contribute to injury, subsets of overactive M2 macrophages are involved in suppressing immune responses and promoting fibrosis (8, 10, 11). The fact that the sequential appearance of activated M1 and M2 macrophages in the lung after NM exposure correlates with early tissue injury and subsequent fibrosis suggests that these cells may contribute to the progression of these pathologies.

A characteristic feature of infiltrating macrophages is expression of CD11b, a cell adhesion molecule important in phagocyte diapedesis (15). We noted a persistent increase in $CD11b^+$ macrophages in histologic sections following NM exposure, indicating the continuous infiltration of inflammatory cells into the lung. However, numbers of $CD11b^+$ macrophages and the intensity of CD11b expression by these cells were reduced 28 days after NM exposure, suggesting that the inflammatory cell influx into the lung was declining during the chronic phase of the injury response. This is supported by our flow cytometric analysis, showing reduced numbers of $CD11b^+$ cells recovered from the lung at this time. The fact that infiltrating $CD11b^+$ cells decreased at a time (28 d) when M2 macrophages increased suggests that at least some populations of M2 macrophages arise from phenotypic switching of M1 macrophages (25).

Acute lung injury induced by NM was associated with increases in $iNOS^+$ M1 macrophages in lung sections within 1 day of exposure. Cells isolated from the lung 1 day after NM also expressed increased levels of iNOS mRNA, as well as other markers of M1 activation, including TNF-α, COX-2, IL-12α, MMP-9, and MMP-10 (10). The observation that $iNOS^+$ M1 macrophages remained in the tissue for at least 28 days and that iNOS, COX-2, IL-12α, and MMP-9 genes were up-regulated for at least 7 days indicates the persistence of a cytotoxic/proinflammatory response. The finding that TNF-α gene expression was transient is consistent with its role as an early response cytokine (26). Proinflammatory/cytotoxic M1 macrophages have been implicated in lung injury induced by ozone and bleomycin, pulmonary toxicants known to cause acute oxidative injury to the lung (27, 28). Additional studies are needed to determine if they play an analogous role in NM-induced acute toxicity.

NM exposure was also associated with a time-related increase in M2 macrophages in histological sections of the lung, characterized by expression of CD68, CD163, CD206, YM-1, or ARG-II. By 28 days, macrophages staining positively for these M2 markers were enlarged, vacuolated, and clustered in thickened alveoli surrounding areas of fibrosis, supporting their profibrotic activity (29, 30). Epidemiological evidence, as well as experimental models of idiopathic and chemical-induced fibrosis, have shown that CD163 and CD206 M2 macrophages contribute to fibrogenesis in the lung, kidney, and peritoneum (31–35). Our findings suggest that they may play a similar role in lung fibrosis after NM exposure; however, this remains to be investigated. We also noted early (1–7 d) up-regulation of IL-10, PTX-2, ApoE, and CTGF gene expression in isolated lung macrophages following NM exposure. Each of these proteins has been shown to play a role in blunting inflammation

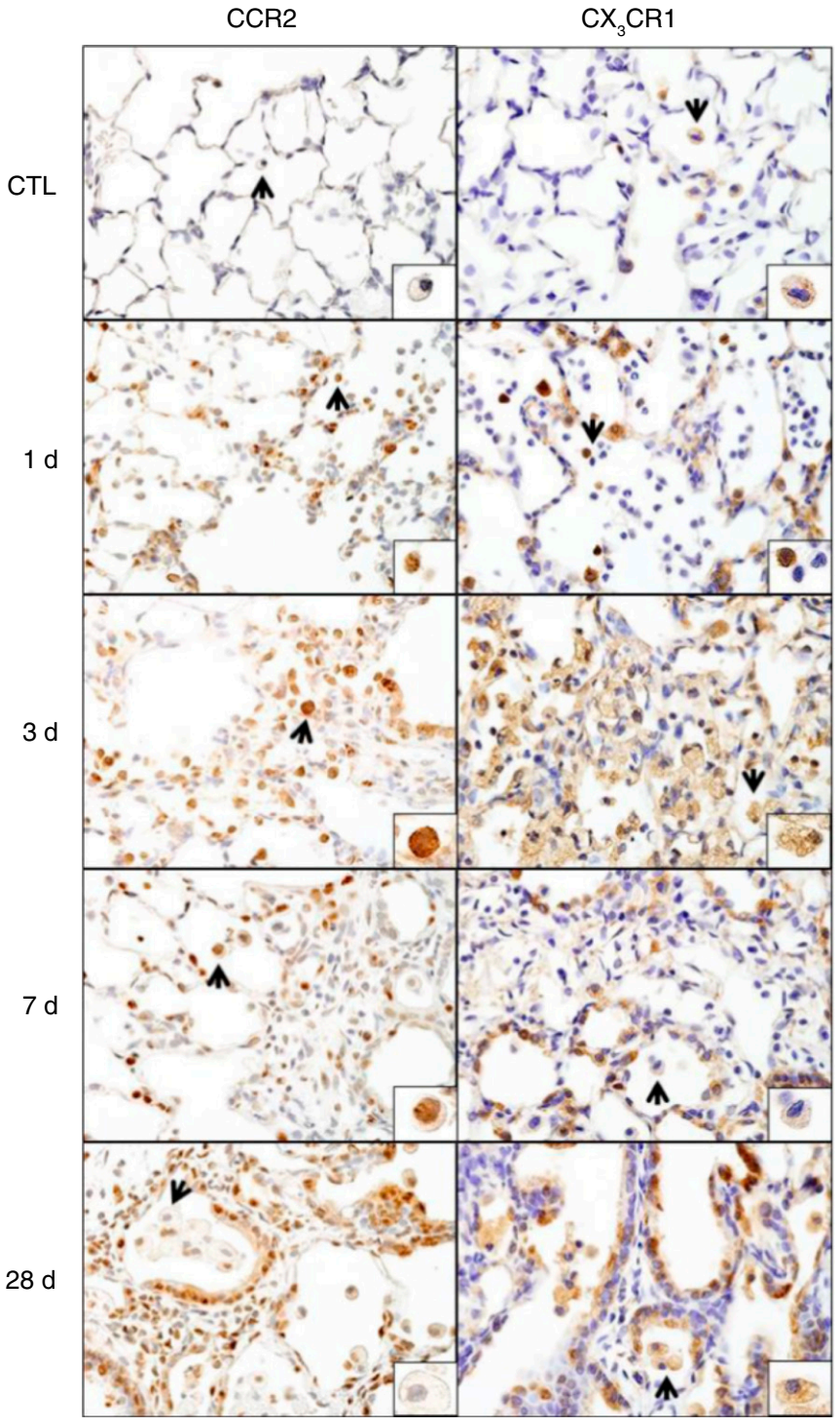

Figure 6. Effects of NM on CCR2 and CX_3CR1 expression. Lung sections, prepared 1, 3, 7, and 28 days after exposure of rats to PBS CTL or NM, were immunostained with antibodies to CCR2 or CX_3CR1. Binding was visualized using a Vectastain kit. *Arrows* indicate macrophage in *insets*. Original magnification, 60×; inset magnification, 200×. Representative sections from three rats/treatment group are shown.

and regulating tissue remodeling and extracellular matrix turnover, characteristics of M2 macrophages (19, 36, 37). The observation that increased numbers of M2 macrophages were present in the lung as early as 1 day after NM and that several M2 genes were up-regulated, indicates that processes associated with tissue repair and fibrogenesis begin early after tissue injury. Previous studies using cultured macrophages have identified three distinct M2 subsets (10): M2a macrophages, which express high levels of CD68, CD163, CD206, and arginase and are involved in type-II immune responses and fibrogenesis; M2b macrophages, which release both proinflammatory (TNF-α, IL-1) and antiinflammatory (IL-10) mediators; and M2c macrophages, which express CD68, CD163, and CD206, as well as YM-1, PTX-2, and ApoE, and function to down-regulate inflammation and initiate tissue remodeling (10, 38, 39). Our findings that $CD68^+$, $CD163^+$, $CD206^+$, and $YM\text{-}1^+$ macrophages appeared in the lung within 1 day of NM exposure, whereas $ARG\text{-}II^+$ macrophages were delayed for 3 days, support the notion that M2 macrophages responding to NM consist of distinct subpopulations. It is tempting to speculate that M2 macrophages identified in histologic sections early after NM are M2a- and M2c-like and function mainly to phagocytize cellular debris and counterbalance M1 cell activation, whereas during the chronic phase (up to 28 d), these macrophages promote matrix deposition, tissue remodeling, and the development of fibrosis. However, at present, experiments designed to test this possibility are limited by a lack of specific reagents available to block different macrophage subsets. Recent studies have suggested that macrophages exist on a continuum, rather than as discrete subpopulations, with no specific genetic signature (9, 40), and this may also reflect their functioning during NM-induced disease pathogenesis.

Heterogeneity within the macrophage populations responding to NM was also analyzed by flow cytometry. The advantage of this analysis is that it allowed us to distinguish between resident ($CD11b^-$) and infiltrating/inflammatory ($CD11b^+$) macrophages. Three distinct subpopulations of cells were identified based on expression of CD11b and CD43 or CD68. These included resident $CD11b^-CD43^-$ and $CD68^+$ macrophages, and two populations of $CD11b^+$ infiltrating macrophages, which were distinguished based on their expression of CD43, a sialoadhesin highly expressed by monocytes and immature macrophage precursors (21). Following NM exposure, numbers of $CD11b^-CD43^-$ resident macrophages

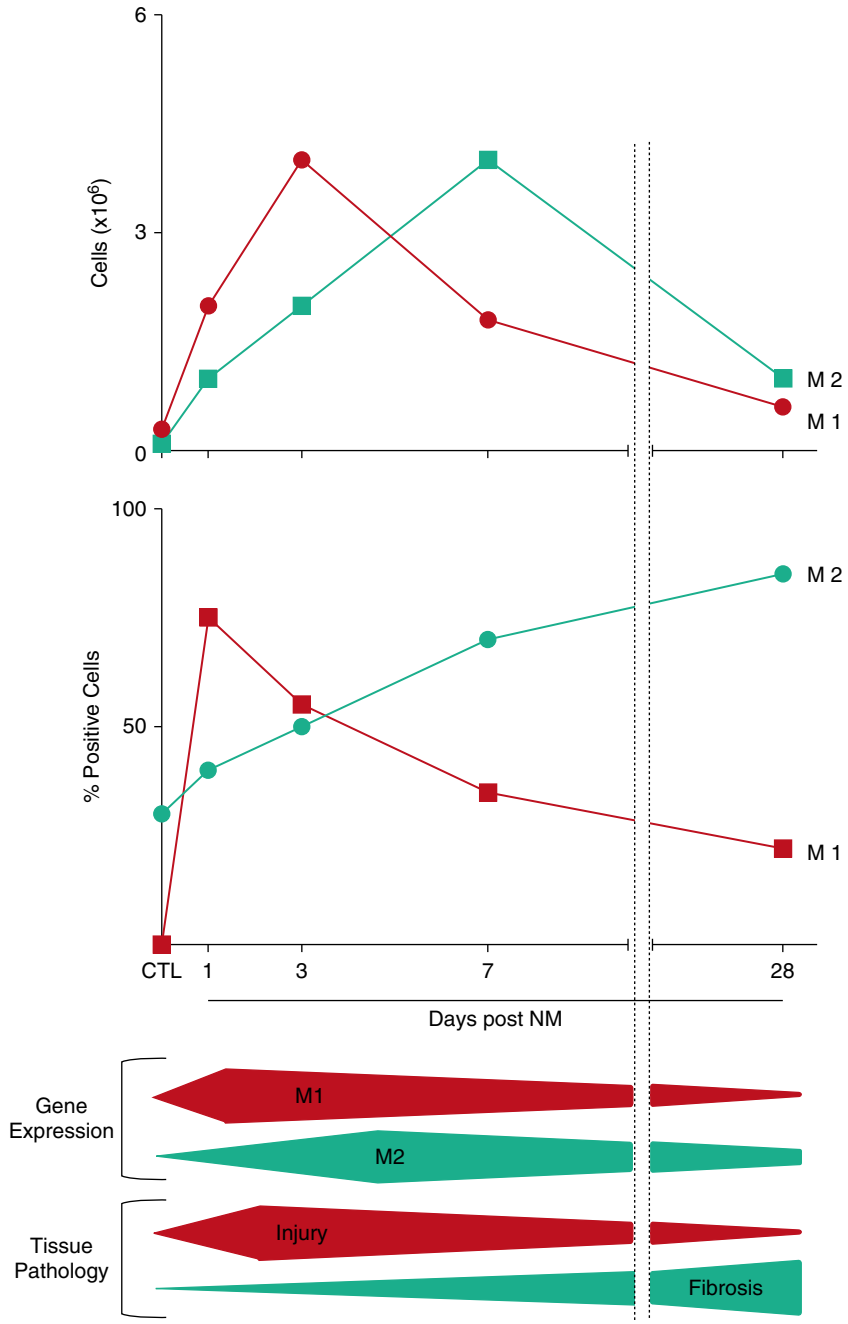

Figure 7. Summary of changes in the lung in response to NM. Following NM exposure, numbers of proinflammatory $CD11b^+CD43^+$ (*upper panel*) and $iNOS^+$ (*middle panel*) M1 macrophages increase transiently, beginning within 1 day; this correlated with up-regulation of M1 genes (iNOS, TNF-α, COX-2, IL-12α, MMP-9, and MMP-10) and tissue injury. Subsequently, $CD11b^+CD43^-$ macrophages accumulate in the lung, a response correlated with up-regulation of M2 genes (IL-10, PTX-2, CTGF, and ApoE). A persistent time-related increase in antiinflammatory/profibrotic $CD68^+$, $CD163^+$, $CD206^+$, ARG-II$^+$, and YM-1^+ M2 macrophages was also observed in the lung after NM (*middle panel*), a response correlated with fibrosis.

decreased for at least 7 days, likely because of direct cytotoxic effects of NM (41, 42). Similar decreases in resident macrophages have been described in the lung, skin, and peritoneum after infection or injury (43–45). By 28 days after NM, resident macrophage numbers were above control levels. Our findings of increased Ki67 expression in these cells suggest that this is caused by the proliferation of residual resident macrophages. This is supported by previous reports of local resident macrophage proliferation in the absence of monocyte influx (46–49).

In contrast to resident macrophages, $CD43^+$ and $CD43^-$ infiltrating ($CD11b^+$) macrophages increased in the lung after NM exposure. Analysis of Ki67 expression in these macrophage subpopulations showed that they both proliferated, indicating that increases in $CD11b^+$ macrophages in the lung after NM exposure are a result of both cellular infiltration and self-renewal. Proliferation of $CD11b^+CD43^+$ and $CD11b^+CD43^-$ macrophages peaked at 3 days and 7 days, respectively, which is consistent with their pattern of accumulation in the lung. These findings are in accord with earlier studies showing increased expression of the proliferation marker proliferating cell nuclear antigen (PCNA) in lung macrophages at 3 days after NM, which remained up-regulated for at least 28 days (6).

Analysis of sorted macrophage subpopulations confirmed their distinct phenotypes. Thus, $CD11b^+CD43^+$ macrophages expressed higher levels of iNOS and IL-12α, when compared with $CD11b^+CD43^-$ cells, suggesting that these cells are polarized toward a proinflammatory M1 phenotype. Conversely, our finding that infiltrating $CD11b^+CD43^-$ macrophages expressed significantly higher levels of IL-10, ApoE, and CX_3CR1, relative to $CD11b^+CD43^+$ macrophages, indicates that these cells are M2 biased. The fact that expression of CD43 was high on M1 macrophages suggests that these cells are more immature and are derived largely from blood monocytes (21). In contrast, low expression of CD43 on $CD11b^+$ M2 macrophages indicates a more mature phenotype. We speculate that these cells are mainly derived from immature M1 macrophages, which develop an M2 phenotype as they mature (25). This is supported by our finding that levels of ApoE, a protein associated with macrophage activation toward an antiinflammatory M2 phenotype (19), were increased 7 days after NM in $CD11b^+CD43^+$ macrophages, relative to $CD11b^+CD43^-$ cells. Similar macrophage maturation and phenotypic switching have been described in renal and

peritoneal models of inflammation (50, 51). Of note, the timing of maximal accumulation of $CD11b^+CD43^+$ macrophages (3 d) and $CD11b^+CD43^-$ macrophages (7 d) in the lung corresponded with peak M1 and M2 macrophage mRNA expression, as well as acute injury, dampening of the proinflammatory response, and fibroplasia (Figure 7). This suggests a potential role of these macrophage subpopulations in the early pathogenic responses to NM; however, this remains to be investigated. Based on differences in the kinetics of their accumulation in the lung, it appears that $CD11b^+CD43^-$ M2 macrophages are distinct from $CD68^+$, $CD163^+$, $CD206^+$, YM-1^+, and ARG-II^+ M2 macrophages, which peak 28 days after NM, and they likely play different roles in NM toxicity. The enlarged vacuolated appearance of the M2 macrophages at 28 days and their location adjacent to fibrotic lesions support the idea that these cells contribute to the fibrogenic process.

The accumulation of M1 and M2 macrophages in the lung correlated with increased expression of the chemokines and chemokine receptors associated with trafficking of M1 (CCL2, CCL5, CCR2, and CCR5) and M2 (fractalkine and CX_3CR1) macrophages to sites of injury (23, 24). A similar correlation in the expression of chemokine receptors and M1/M2 macrophage accumulation has been described in models of bleomycin-induced lung fibrosis and lung cancer, as well as in skin fibrosis and atherosclerosis (52–55). Increased expression of both M1 and M2 chemokines 1–7 days after NM exposure suggests that early in the pathogenic process, the lung actively recruits both macrophage subtypes to the sites of injury. This is supported by our findings of increased numbers of pro- and antiinflammatory macrophages expressing M1 and M2 chemokine receptors in the lung 1–7 days after NM. These data suggest that chemokines and chemokine receptors may be potential pharmacological targets for reducing lung inflammation, injury, and fibrosis.

Conclusions

NM-induced injury is associated with a complex cascade of events, including acute inflammation, tissue injury, remodeling, and fibrosis. The current studies show that after NM exposure, M1 macrophages accumulate in the lung, followed by M2 macrophage subsets. These cells are known to regulate pathogenic responses to a variety of pulmonary toxicants (8, 12). Further studies are required to determine if they contribute to NM-induced lung pathologies. Elucidating the phenotype of macrophages accumulating in the lung after NM exposure, the mechanisms mediating their recruitment, and their specific role in toxicity are important for the development of targeted clinical therapies aimed at blunting macrophage activation and mitigating NM-induced injury. ■

Author disclosures are available with the text of this article at www.atsjournals.org.

Acknowledgments: The authors thank David Reimer, D.V.M., for performing all PBS and nitrogen mustard instillations.

References

1. Dacre JC, Goldman M. Toxicology and pharmacology of the chemical warfare agent sulfur mustard. *Pharmacol Rev* 1996;48: 289–326.
2. Ghabili K, Agutter PS, Ghanei M, Ansarin K, Panahi Y, Shoja MM. Sulfur mustard toxicity: history, chemistry, pharmacokinetics, and pharmacodynamics. *Crit Rev Toxicol* 2011;41:384–403.
3. Ghanei M, Naderi M, Kosar AM, Harandi AA, Hopkinson NS, Poursaleh Z. Long-term pulmonary complications of chemical warfare agent exposure in Iraqi Kurdish civilians. *Inhal Toxicol* 2010;22:719–724.
4. Weinberger B, Laskin JD, Sunil VR, Sinko PJ, Heck DE, Laskin DL. Sulfur mustard-induced pulmonary injury: therapeutic approaches to mitigating toxicity. *Pulm Pharmacol Ther* 2011;24:92–99.
5. Malaviya R, Sunil VR, Cervelli J, Anderson DR, Holmes WW, Conti ML, Gordon RE, Laskin JD, Laskin DL. Inflammatory effects of inhaled sulfur mustard in rat lung. *Toxicol Appl Pharmacol* 2010;248:89–99.
6. Malaviya R, Venosa A, Hall L, Gow AJ, Sinko PJ, Laskin JD, Laskin DL. Attenuation of acute nitrogen mustard-induced lung injury, inflammation and fibrogenesis by a nitric oxide synthase inhibitor. *Toxicol Appl Pharmacol* 2012;265:279–291.
7. Sunil VR, Vayas KN, Cervelli JA, Malaviya R, Hall L, Massa CB, Gow AJ, Laskin JD, Laskin DL. Pentoxifylline attenuates nitrogen mustard-induced acute lung injury, oxidative stress and inflammation. *Exp Mol Pathol* 2014;97:89–98.
8. Laskin DL, Sunil VR, Gardner CR, Laskin JD. Macrophages and tissue injury: agents of defense or destruction? *Annu Rev Pharmacol Toxicol* 2011;51:267–288.
9. Mosser DM, Edwards JP. Exploring the full spectrum of macrophage activation. *Nat Rev Immunol* 2008;8:958–969.
10. Martinez FO, Gordon S. The M1 and M2 paradigm of macrophage activation: time for reassessment. *F1000Prime Rep* 2014;6:13.
11. Sica A, Mantovani A. Macrophage plasticity and polarization: in vivo veritas. *J Clin Invest* 2012;122:787–795.
12. Murray PJ, Wynn TA. Protective and pathogenic functions of macrophage subsets. *Nat Rev Immunol* 2011;11:723–737.
13. Sunil VR, Patel KJ, Shen J, Reimer D, Gow AJ, Laskin JD, Laskin DL. Functional and inflammatory alterations in the lung following exposure of rats to nitrogen mustard. *Toxicol Appl Pharmacol* 2011;250:10–18.
14. Kirby AC, Raynes JG, Kaye PM. CD11b regulates recruitment of alveolar macrophages but not pulmonary dendritic cells after pneumococcal challenge. *J Infect Dis* 2006; 193:205–213.
15. Chamoto K, Gibney BC, Lee GS, Ackermann M, Konerding MA, Tsuda A, Mentzer SJ. Migration of CD11b+ accessory cells during murine lung regeneration. *Stem Cell Res (Amst)* 2013;10:267–277.
16. Zaynagetdinov R, Sherrill TP, Kendall PL, Segal BH, Weller KP, Tighe RM, Blackwell TS. Identification of myeloid cell subsets in murine lungs using flow cytometry. *Am J Respir Cell Mol Biol* 2013;49: 180–189.
17. Huang WC, Sala-Newby GB, Susana A, Johnson JL, Newby AC. Classical macrophage activation up-regulates several matrix metalloproteinases through mitogen activated protein kinases and nuclear factor-κB. *PLoS One* 2012;7:e42507.
18. Blom IE, Goldschmeding R, Leask A. Gene regulation of connective tissue growth factor: new targets for antifibrotic therapy? *Matrix Biol* 2002;21:473–482.
19. Baitsch D, Bock HH, Engel T, Telgmann R, Müller-Tidow C, Varga G, Bot M, Herz J, Robenek H, von Eckardstein A, *et al*. Apolipoprotein E induces antiinflammatory phenotype in macrophages. *Arterioscler Thromb Vasc Biol* 2011;31:1160–1168.
20. Davies LC, Jenkins SJ, Allen JE, Taylor PR. Tissue-resident macrophages. *Nat Immunol* 2013;14:986–995.
21. Howell DN, Ahuja V, Jones L, Blow O, Sanfilippo FP. Differential expression of CD43 (leukosialin, sialophorin) by mononuclear phagocyte populations. *J Leukoc Biol* 1994;55:536–544.
22. Kee N, Sivalingam S, Boonstra R, Wojtowicz JM. The utility of Ki-67 and BrdU as proliferative markers of adult neurogenesis. *J Neurosci Methods* 2002;115:97–105.

23. Mantovani A, Savino B, Locati M, Zammataro L, Allavena P, Bonecchi R. The chemokine system in cancer biology and therapy. *Cytokine Growth Factor Rev* 2010;21:27–39.
24. Ingersoll MA, Platt AM, Potteaux S, Randolph GJ. Monocyte trafficking in acute and chronic inflammation. *Trends Immunol* 2011;32:470–477.
25. Arnold L, Henry A, Poron F, Baba-Amer Y, van Rooijen N, Plonquet A, Gherardi RK, Chazaud B. Inflammatory monocytes recruited after skeletal muscle injury switch into antiinflammatory macrophages to support myogenesis. *J Exp Med* 2007;204: 1057–1069.
26. Moldoveanu B, Otmishi P, Jani P, Walker J, Sarmiento X, Guardiola J, Saad M, Yu J. Inflammatory mechanisms in the lung. *J Inflamm Res* 2009;2:1–11.
27. Fakhrzadeh L, Laskin JD, Laskin DL. Deficiency in inducible nitric oxide synthase protects mice from ozone-induced lung inflammation and tissue injury. *Am J Respir Cell Mol Biol* 2002;26:413–419.
28. Genovese T, Cuzzocrea S, Di Paola R, Failla M, Mazzon E, Sortino MA, Frasca G, Gili E, Crimi N, Caputi AP, *et al*. Inhibition or knock out of inducible nitric oxide synthase result in resistance to bleomycin-induced lung injury. *Respir Res* 2005;6:58.
29. Boven LA, Van Meurs M, Van Zwam M, Wierenga-Wolf A, Hintzen RQ, Boot RG, Aerts JM, Amor S, Nieuwenhuis EE, Laman JD. Myelin-laden macrophages are anti-inflammatory, consistent with foam cells in multiple sclerosis. *Brain* 2006;129:517–526.
30. van Tits LJ, Stienstra R, van Lent PL, Netea MG, Joosten LA, Stalenhoef AF. Oxidized LDL enhances pro-inflammatory responses of alternatively activated M2 macrophages: a crucial role for Krüppel-like factor 2. *Atherosclerosis* 2011;214:345–349.
31. Stahl M, Schupp J, Jäger B, Schmid M, Zissel G, Müller-Quernheim J, Prasse A. Lung collagens perpetuate pulmonary fibrosis via CD204 and M2 macrophage activation. *PLoS One* 2013;8:e81382.
32. Pechkovsky DV, Prasse A, Kollert F, Engel KM, Dentler J, Luttmann W, Friedrich K, Müller-Quernheim J, Zissel G. Alternatively activated alveolar macrophages in pulmonary fibrosis-mediator production and intracellular signal transduction. *Clin Immunol* 2010;137:89–101.
33. Bellón T, Martínez V, Lucendo B, del Peso G, Castro MJ, Aroeira LS, Rodríguez-Sanz A, Ossorio M, Sánchez-Villanueva R, Selgas R, *et al*. Alternative activation of macrophages in human peritoneum: implications for peritoneal fibrosis. *Nephrol Dial Transplant* 2011;26: 2995–3005.
34. Lu J, Cao Q, Zheng D, Sun Y, Wang C, Yu X, Wang Y, Lee VW, Zheng G, Tan TK, *et al*. Discrete functions of M2a and M2c macrophage subsets determine their relative efficacy in treating chronic kidney disease. *Kidney Int* 2013;84:745–755.
35. Ikezumi Y, Suzuki T, Yamada T, Hasegawa H, Kaneko U, Hara M, Yanagihara T, Nikolic-Paterson DJ, Saitoh A. Alternatively activated macrophages in the pathogenesis of chronic kidney allograft injury. *Pediatr Nephrol* 2015;30:1007–1017.
36. Castaño AP, Lin SL, Surowy T, Nowlin BT, Turlapati SA, Patel T, Singh A, Li S, Lupher ML Jr, Duffield JS. Serum amyloid P inhibits fibrosis through FcγR dependent monocyte-macrophage regulation in vivo. *Sci Transl Med* 2009;1:5ra13.
37. Ponticos M, Holmes AM, Shi-wen X, Leoni P, Khan K, Rajkumar VS, Hoyles RK, Bou-Gharios G, Black CM, Denton CP, *et al*. Pivotal role of connective tissue growth factor in lung fibrosis: MAPK-dependent transcriptional activation of type I collagen. *Arthritis Rheum* 2009;60: 2142–2155.
38. Moestrup SK, Møller HJ. CD163: a regulated hemoglobin scavenger receptor with a role in the anti-inflammatory response. *Ann Med* 2004;36:347–354.
39. Zhou Y, Peng H, Sun H, Peng X, Tang C, Gan Y, Chen X, Mathur A, Hu B, Slade MD, *et al*. Chitinase 3-like 1 suppresses injury and promotes fibroproliferative responses in mammalian lung fibrosis. *Sci Transl Med* 2014;6:240ra76.
40. Hume DA, Freeman TC. Transcriptomic analysis of mononuclear phagocyte differentiation and activation. *Immunol Rev* 2014;262: 74–84.
41. Barth MW, Hendrzak JA, Melnicoff MJ, Morahan PS. Review of the macrophage disappearance reaction. *J Leukoc Biol* 1995;57: 361–367.
42. Rappeneau S, Baeza-Squiban A, Jeulin C, Marano F. Protection from cytotoxic effects induced by the nitrogen mustard mechlorethamine on human bronchial epithelial cells in vitro. *Toxicol Sci* 2000;54: 212–221.
43. Davies LC, Rosas M, Jenkins SJ, Liao CT, Scurr MJ, Brombacher F, Fraser DJ, Allen JE, Jones SA, Taylor PR. Distinct bone marrow-derived and tissue-resident macrophage lineages proliferate at key stages during inflammation. *Nat Commun* 2013;4:1886.
44. Kirby AC, Coles MC, Kaye PM. Alveolar macrophages transport pathogens to lung draining lymph nodes. *J Immunol* 2009;183: 1983–1989.
45. Lauder SN, Taylor PR, Clark SR, Evans RL, Hindley JP, Smart K, Leach H, Kidd EJ, Broadley KJ, Jones SA, *et al*. Paracetamol reduces influenza-induced immunopathology in a mouse model of infection without compromising virus clearance or the generation of protective immunity. *Thorax* 2011;66:368–374.
46. Côté CH, Bouchard P, van Rooijen N, Marsolais D, Duchesne E. Monocyte depletion increases local proliferation of macrophage subsets after skeletal muscle injury. *BMC Musculoskelet Disord* 2013;14:359.
47. Davies LC, Rosas M, Smith PJ, Fraser DJ, Jones SA, Taylor PR. A quantifiable proliferative burst of tissue macrophages restores homeostatic macrophage populations after acute inflammation. *Eur J Immunol* 2011;41:2155–2164.
48. Hashimoto D, Chow A, Noizat C, Teo P, Beasley MB, Leboeuf M, Becker CD, See P, Price J, Lucas D, *et al*. Tissue-resident macrophages self-maintain locally throughout adult life with minimal contribution from circulating monocytes. *Immunity* 2013;38: 792–804.
49. Jenkins SJ, Ruckerl D, Cook PC, Jones LH, Finkelman FD, van Rooijen N, MacDonald AS, Allen JE. Local macrophage proliferation, rather than recruitment from the blood, is a signature of TH2 inflammation. *Science* 2011;332:1284–1288.
50. Lin SL, Castaño AP, Nowlin BT, Lupher ML Jr, Duffield JS. Bone marrow Ly6Chigh monocytes are selectively recruited to injured kidney and differentiate into functionally distinct populations. *J Immunol* 2009;183:6733–6743.
51. Liu G, Ma H, Qiu L, Li L, Cao Y, Ma J, Zhao Y. Phenotypic and functional switch of macrophages induced by regulatory CD4+CD25+ T cells in mice. *Immunol Cell Biol* 2011;89:130–142.
52. Arai M, Ikawa Y, Chujo S, Hamaguchi Y, Ishida W, Shirasaki F, Hasegawa M, Mukaida N, Fujimoto M, Takehara K. Chemokine receptors CCR2 and CX3CR1 regulate skin fibrosis in the mouse model of cytokine-induced systemic sclerosis. *J Dermatol Sci* 2013;69:250–258.
53. Okuma T, Terasaki Y, Kaikita K, Kobayashi H, Kuziel WA, Kawasuji M, Takeya M. C-C chemokine receptor 2 (CCR2) deficiency improves bleomycin-induced pulmonary fibrosis by attenuation of both macrophage infiltration and production of macrophage-derived matrix metalloproteinases. *J Pathol* 2004;204:594–604.
54. Schmall A, Al-Tamari HM, Herold S, Kampschulte M, Weigert A, Wietelmann A, Vipotnik N, Grimminger F, Seeger W, Pullamsetti SS, *et al*. Macrophage and cancer cell cross-talk via CCR2 and CX3CR1 is a fundamental mechanism driving lung cancer. *Am J Respir Crit Care Med* 2015;191:437–447.
55. Tacke F, Alvarez D, Kaplan TJ, Jakubzick C, Spanbroek R, Llodra J, Garin A, Liu J, Mack M, van Rooijen N, *et al*. Monocyte subsets differentially employ CCR2, CCR5, and CX3CR1 to accumulate within atherosclerotic plaques. *J Clin Invest* 2007;117:185–194.